MOLECULAR PHYSICS REPORTS 9 (1995) 92-116

INVARIANT MEASURES WITH QUASICRYSTALLINE SYMMETRY GENERATED BY ITERATED FUNCTION SYSTEMS

PIOTR PIERAŃSKI[1], RICCARDO BARBERI[2], JAROSŁAW KŁOS[1]

[1] *Institute of Molecular Physics, Smoluchowskiego 17, 60 179 Poznań, Poland*
[2] *University of Calabria, Department of Physics, 87 036 Arcavacata di Rende, Italy*

1. INTRODUCTION

In spite of what most readers would most probably claim, the image presented in Fig. 1 is not a photograph of the diffraction pattern of a quasicrystalline structure – it is a computer graphics image of the attractor of a particular iterated function system. It is the apparent similarity of these two objects that made us to perform the study described below.

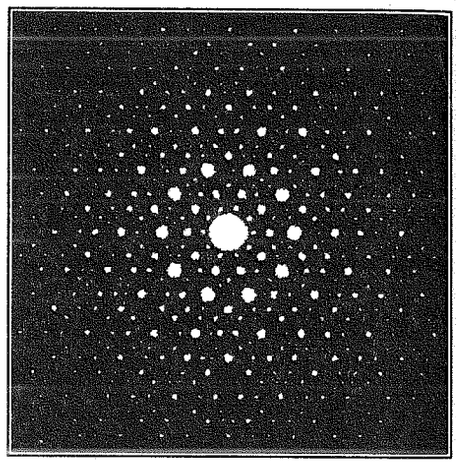

Fig. 1. A computer graphics image of an invariant measure of a particular iterated function system with probabilities.

The main aim of it was to make a reconnaissance tour into those parts of the theory of the iterated function systems where quasicrystalline structures can be found. The tour is far from being completed, but since results we obtained seem to be interesting, we dare to present them.

Since most readers are more familiar with quasicrystals than with iterated function systems, the main emphasis of the introductory part of the present paper will be devoted to the latter. It seems to us that such a physics oriented introduction can be of a use for many readers; original literature on the theory of the iterated function systems

is rather difficult to read. Avoiding any simplifications, we shall try to make the theory as transparent as possible. The price paid for it will be omission of formal proofs.

2. ITERATED FUNCTION SYSTEMS AND THE RANDOM ITERATION ALGORITHM

Reading today the already classical *Fractals: Form, Chance, Dimension* by Benoit Mandelbrot [1] one is still amazed by the apparently non-exhaustible richness of forms which fractal objects may take. No doubt, the fast and overwhelming success of Mandelbrot ideas is in a great part due to the beauty of the graphical shape of the first book on the subject. There must have been a lot of hard program writing to produce all the high resolution pictures. Yet today most of them can be reproduced without too much effort by a single numerical tool: the *random iteration algorithm* (RIA) developed by Barnsley [2]. To convince the reader that these are not but empty words we dare to present Fig. 2 [3]. All pictures present computer graphics images of the invariant measures of some iterated function systems with probabilities. They prove, we hope, that the technique of iterated function systems is very powerful. It allows one to create images very similar to many complex objects seen in nature. What we want to demonstrate in the present paper is that the quasicrystalline patterns are among them.

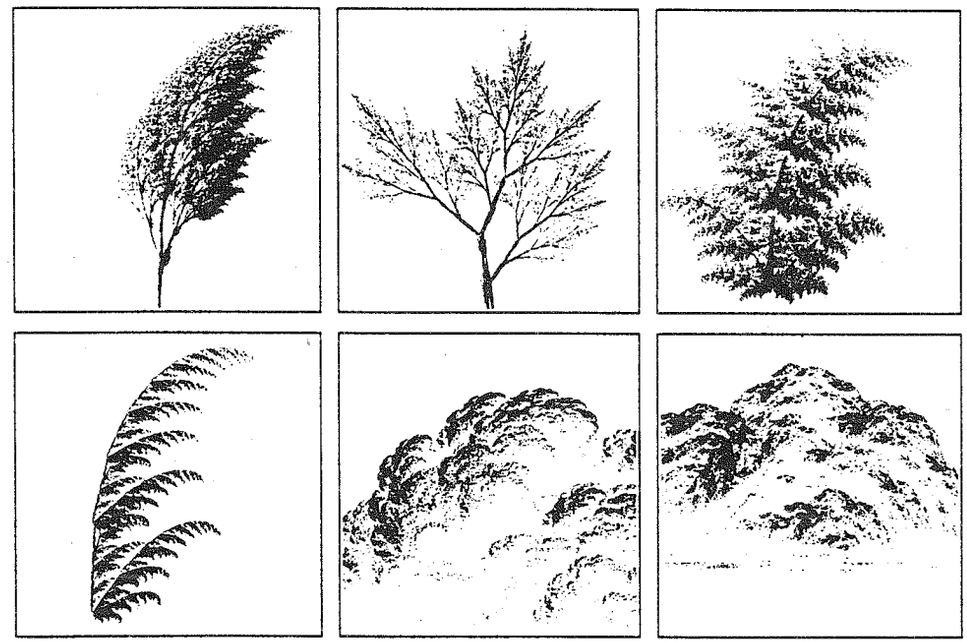

Fig. 2. Computer graphics images of the invariant measures of a few iterated function systems with probabilities.

In what follows we shall describe in brief the basic structure of the theory of the iterated function systems. Its detailed exposition can be found, among others in Ref [2]. Presenting a few basic theorems on which the random iteration algorithm is based we shall provide them with comments expressed in terms of the computer graphics procedures. It seems that the gap between the languages of the measure theory, in which the theorems are formulated, and that of the practical computer programming is large enough to confuse many possible users of iterated function systems.

Most fractals, of which one would start thinking when asked to tell a few words on the subject, are subsets of the two dimensional Euclidean plane R^2. To fix attention, we shall be staying in all examples presented below within this topological dimension but in general the metric space, where all the iterated function theory works, may be of any dimension and nature.

Let (X, d) be a complete metric space e.g. a two dimensional plane R^2 with Euclidean metric. Let $A.IFS = \{w_1, w_2, w_3,..., w_n\}$ be a set of contractive transformations defined within (X, d), i.e. for any w_α, $\alpha = 1, 2,..., n$, there exists $s \in R$, $0 \le s < 1$, such that for any $x, y \in X$

$$d(w_\alpha(x), w_\alpha(y)) \le sd(x, y) \tag{1}$$

A.IFS defined in this manner is called a *hyperbolic iteration function system.*

Iterated function systems are used as means of transportation within the abstract space $H(X)$ whose elements are compact subsets of X. Starting a travel within any space is better to know how to measure the distances within it. Below, we define such a tool for $H(X)$.

2.1 Iterated Function Systems

Definition 2.1

Let $H(X)$ be the space of all compact subsets of X. It can be equipped by a Hausdorff metric h. Its definition goes in three steps.

1. One defines the distance between a point and a subset:

$$d_1(x, B) = \min_y \{d(x, y): y \in B\} \tag{2}$$

2. One defines the distance from one subset to another subset:

$$d_2(A, B) = \max_x \{d_1(x, B): \in A\} \tag{3}$$

(A wolf caged within set B tries to catch a sheep locked within meadow B. The closest distance the wolf can reach to the refuge seeking sheep is equal to $d_2(A, B)$. [4])

3. Distance d_2 thus defined is not symmetrical. The final step of the definition removes this fault:

$$h(A, B) = \max\{d_2(A, B), d_2(B, A)\} \tag{4}$$

Space $H(X)$ equipped with metric h is complete. Thus, any Cauchy sequence of compact subsets of X finds its limit within the space. Equation:

$$W_F(A) = w_1(A) \cup w_2(A) \cup ... \cup w_n(A), \tag{5}$$

where all transformations $w_\alpha \in F.IFS$, $\alpha = 1, 2,..., n$, are contractive, defines within $H(X)$ transformation W_F which can be shown to be contractive as well. See Ref. [2] p. 82. Being contractive, it is continuous and has a unique fixed point F within $H(X)$ which, by definition, stays invariant under the action of W_F

$$W_F(F) = F \tag{6}$$

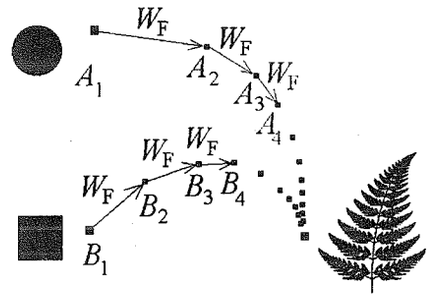

Fig. 3. All roads lead to Rome.

Set F is said to be the *attractor* of *F.IFS*. Since F belongs to $H(X)$, it is a compact subset of X. How to find it? Starting from any compact subset G_0 and applying in an iterative manner transformation W_F

$$G_{i+1} = W_F(G_i) \tag{7}$$

one produces a Cauchy sequence $G_0, G_1, G_2,...$ of compact sets which converge to F. See Fig. 3. Since $H(X)$ is complete, the limit also belongs to the space. This is the essence of the beauty and efficiency of the iterated function system algorithm. Changing parameters of transformations within an IFS one may reach within space $H(X)$ places of incredible beauty. The book by Barnsley makes the first guide to them.

2.2 Random Iteration Algorithm

The IFS algorithm in its original form allows one to produce "black-and white" pictures of fractal sets. A point of space is, say, black when it belongs to the attractor of the IFS or, it is white when it does not belong to it. Yet, as we may easily see looking through the window, real objects, even if of fractal structure, are not black and white. Even a black and white photograph of an X-ray diffraction pattern of a crystal proves that the latter is not black and white: its Bragg diffraction spots are not either single points nor finite size circles. They are smooth, rapidly decaying functions, localised with their maxima at well defined points and spreading with their tails through the whole plane of the picture. The diffraction pattern $D(x, y)$ is a sum of such

functions. Any photograph deforms strongly their height distribution: high intensity diffraction spots make whole circular parts of the photograph film practically black while those of a very weak intensity do not manage to leave even a single trace on it. This is particularly well visible in the photographs of the diffraction patterns of the quasicrystals for which the set of points on which the Bragg spots are localised should be dense in plane, yet the final contrast ability of the photographic film allows one to record but a final subset of it.

The black-and-white technique of the IFS algorithm may be used to reproduce the silhouettes of many complex objects, but to mimic their grey shadow structure the algorithm must be extended. See Fig. 4. The random iteration algorithm makes such an extension. This is how it works.

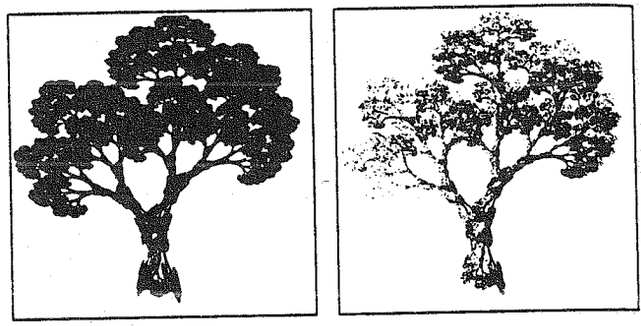

Fig. 4. Attractor of an IFS (on the left) and the invariant measure of the same IFS with probabilities.

In addition to the set of contraction transformations $\{w_1, w_2, w_3, \ldots w_n\}$ of an *A.IFS* one defines a set of real numbers $\{p_1, p_2, p_3, \ldots, p_n\}$ such that $p_1 + p_2 + p_3 + \ldots + p_n = 1$. The set $\{w_1, w_2, w_3, \ldots w_n, p_1, p_2, p_3, \ldots, p_n\}$ will be called *an iterated function system with probabilities* and we shall denote it by *A.IFSP*.

Let $A \in X$ be the attractor of an $A.IFS = \{w_1, w_2, w_3, \ldots w_n, p_1, p_2, p_3, \ldots, p_n\}$. Let x_0 be a point belonging to A. The following iterative procedure can be applied (we define below its i-th step):

RIA 1. One of the $\{w_1, w_2, w_3, \ldots w_n\}$ transformation is chosen, say $w_{\alpha i}$, with a probability given by $p_{\alpha i}$.

RIA 2. Point x_{i-1} is transformed into point $x_i = w_{\alpha i}(x_{i-1})$.

Since, by assumption, the starting point x_0 belongs to the attractor A, all following points $x_1, x_2, \ldots, x_i, \ldots$ generated by the procedure will also belong to it. (If x_0 is not the member of A, then the consecutive points $x_1, x_2, \ldots, x_i, \ldots$ will, in general, also be not members of the attractor. Since, however, transformations of A are contractive, the points will rapidly converge to it and, in view of the finite resolution of any technical means by which they can be visualised, they may be presented as belonging to A.)

Let us see, how the random iteration algorithm works in the case of the simplest IFS which defines (as its attractor) a square. Let us denote such an IFS as ■.IFS. The

■.IFS consists of four affine transformations $\{w_1, w_2, w_3, w_4\}$ each of which transforms the square into one of its four quarters. See Fig. 5.

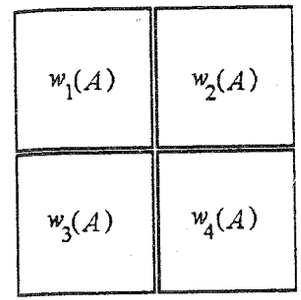

Fig. 5. Square A can be seen as a sum of four of its copies obtained by application of four affine transformations $\{w_1, w_2, w_3, w_4\}$.

To initiate the random iteration procedure we choose a single point e.g. $P_0 = (0, 0)$, one of the four transformations $\{w_1, w_2, w_3, w_4\}$ is chosen at random and point P_0 is transformed into P_1. Then the choose-and-transform procedure is repeated in the iterative manner. Fig. 6 presents frames taken from the computer graphics display during the iteration process.

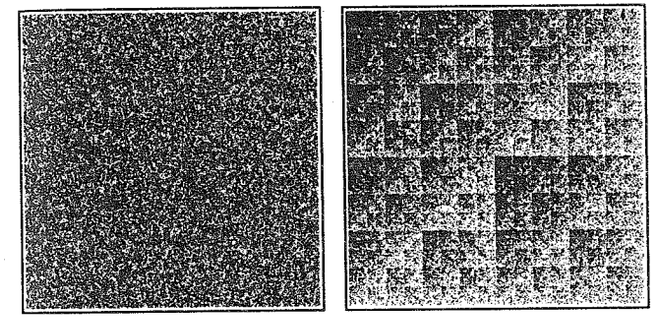

Fig. 6. First 100000 points produced by the random iteration algorithm for the ■.IFS described in the text. $p_1 = p_2 = p_3 = p_4 = 0.25$ for the image shown on the left; $p_1 = 0{,}4$, $p_2 = p_3 = p_4 = 0.2$ for that on the right.

In the particular iteration sequence presented on the left of the figure the probabilities p_1, p_2, p_3 and p_4, with which the four transformations w_1, w_2, w_3 and w_4 were chosen, were equal. One can see that as a result the iteration procedure was producing points which covered the square in a uniform manner.

The image changes radically, when the four probabilities are not equal to each other. See right part of Fig. 6. Here, the density of the cloud of points produced by the iteration procedure is no more uniform but displays a very intricate structure which reflects the non uniformity of the process in which the transformation of the IFS were chosen during the iteration procedure. Each set of probabilities $\{p_1, p_2, p_3, p_4\}$ determines its own characteristic density pattern over the square A. (We use the term "density" in a heuristic manner. Since attractors of iterated function systems display in general fractal structure, the densities of which we shall be talking may strongly

differ from what an experimentalist would usually mean. If one thinks of the density of something material, e.g. a mass, spread within a 2D Euclidean space X then one must take into account also such singular forms of it as a linear and point masses. To describe such densities in a formal manner one must use the concept of the generalised functions (distributions) e.g. the Dirac delta function.) As the iteration procedure continues, the pattern becomes better visible, more and more fine details of it are appearing on the computer display; unfortunately, the finite pixel size of any computer graphics display puts an inevitable end to this process. Below we shall discuss the problem in more detail.

In the previous paragraph attractors of iterated function systems were shown to make fixed points of contraction transformations which the systems define in the space $(H(X), \mathrm{h})$ of compact subsets of X equipped with the Hausdorff metric. In the same manner, any IFSP will be shown below to define its own "density pattern", as a fixed point of a contraction transformation within the space of all such patterns. Let us present a very brief outline of the mathematical formalism within which the above statement can be formulated and proven.

Let (X, d) be a compact metric space. Let $P(X)$ be the set of normalised Borel measures on X. (If one thinks in terms of computer graphics images printed with a laser printer of infinite resolution on a piece of paper, then X can be thought of as the surface of the paper while $P(X)$ will be the set of all possible patterns one can print on it using toner of a unit mass.) The $P(X)$ space can be equipped with a metric i.e. a tool which not only allows one to tell one pattern from another, but also to determine in a quantitative manner *how much* they are different.

Let $G(X)$ be the set of all continuous, real valued functions g such that for all x, $y \in X$, $|g(x) - g(y)| \leq d(x, y)$.

Definition. 2.2.

The Hutchinson metric d_H on $P(X)$ is defined by:

$$d_H(\mu, \nu) = \sup_{g \in G} \left\{ \int_X g\,d\mu - \int_X g\,d\nu \right\} \tag{8}$$

Remark

Returning once more to the technical terminology of computer graphics the definition of the Hutchinson metric can be interpreted as follows. Having two different patterns ○ and □, both printed with the unit mass of toner (in a technique which allows to obtain the whole continuous range of the grey shadows) we want to find a single number which would tell how much they are different. A possible way of

achieving the goal is to put the two patterns into two identical optical systems which project them onto two photodiodes and measure the integrated optical density of the patterns. Obviously, since the amount of toner used to draw both patterns was equal, such a measure would show identical values. This is the proof that the patterns are normalised. To reveal the difference between them, we cover the patterns with a pair of identical optical filters, e.g. glass plates with smooth (limited density gradient!) grey shadow design fused into them, and perform once more the measure of the integrated optical density. With the exception of some singular cases, such a measure will produce two different numbers if only ○ and □ are different. The problem is to find such a pair of identical filters for which the difference will be the largest one.

One can prove that the space of measures $P(X)$ equipped with such a metric is also compact. As discussed in the previous part, contractive transformations defined in space X transform compact sets into compact sets. What happens to measures during such transformations?

Let w be such a contractive transformation and w^{-1} be its inverse. (We assume the inverse exists, which is not automatic.) If μ is a normalised Borel measure on X, i.e. $\mu \in P(X)$, then μ_w defined by equation:

$$\mu_w(A) = \mu(w^{-1}(A)) \tag{9}$$

is also a normalised Borel measure on X i.e. it belongs to $P(X)$.

Let $A.IFSP = \{w_1, w_2, w_3, \ldots w_n, p_1, p_2, p_3, \ldots, p_n\}$ be an IFS with probabilities.

Definition 2.3

The *Markov operator M_A associated with A.IFSP* is defined by the formula: M_A: $\mu \rightarrow \nu = M_A(\mu)$ such that

$$\nu(S) = p_1\mu(w_1^{-1}(S)) + p_2\mu(w_2^{-1}(S)) + \ldots + p_n\mu(w_n^{-1}(S)) \tag{10}$$

where S is an arbitrary Borel set.

If μ is a normalised Borel measure, then is a normalised Borel measure as well. Thus the Markov operator transforms any the $P(X)$ space into itself. One can prove that if all transformations $\{w_1, w_2, w_3, \ldots w_n\}$ of an *A.IFSP* are contractive within X then the Markov operation M_A is also contractive in $P(X)$. Contractivity factors of *A.IFS* and M_A are equal.

Being contractive, mapping M_A is continuous. It has a unique fixed point within $P(X)$ i.e. there exists a normalised Borel measure, let us denote it by μ_A such that

$$M_A(\mu_A) = \mu_A \tag{11}$$

i.e. it stays invariant under the application of the Markov operator associated with *A.IFSP*.

Which is the relation between the attractor of *A.IFS* and that of *A.IFSP*? The former one, A, is a subset of X, while the latter one, μ_A, is a measure defined within the same space; A is the support of μ_A. The Barnsley random iteration algorithm allows one to visualise both. If one runs it on a digital computer, displaying consecutive points on a graphics display, the image which appears becomes better and better visible. It strongly reminds the photographic development process. If the first point with which the iteration procedure starts belongs to A, so will the all of them. They cover A with a density proportional to μ_A. This phenomenon is described in a precise manner by the Elton's theorem and its corollary. See Ref. [2] p. 370.

Theorem 2.1

Let $A.IFSP = \{w_1, w_2, ..., w_n; p_1, p_2, ..., p_n\}$ be an iterated function system with probabilities defined with a compact metric space (X, d). Let $x_0, x_1, x_2, ...$ be a sequence of points produced by the random iteration algorithm applied to *A.IFSP*. Let μ_A be the invariant measure for *A.IFSP*. Then, with probability one the following holds:

$$\lim_{n\to\infty} \frac{1}{n+1} \sum_{k=1} f(x_k) = \int_X f(x)\, d\mu_A(x) \tag{12}$$

for all continuous functions $f: X \to R$ and all x_0

Corollary.

Let B be a Borel subset of X such that its boundary ∂B is of measure zero i.e. $\mu_A(\partial B) = 0$. Let $N(B, n)$ be the number of those points from the sequence $x_0, x_1, x_2, ..., x_n$ defined above which fall into B. Then, with probability one

$$\mu_A(B) = \lim_{n\to\infty} \frac{N(B,n)}{n+1} \tag{13}$$

for all starting points x_0.

Obvious limits put on the process of this decoration are the accuracy of the computer and the finite size of pixels of any graphical display. One must be aware that in view of the second factor, the image of the invariant measure may become less visible also when the run time is too long. Assuming that the plotted picture is black and white, it will inevitably loose in the end its density structure; all points belonging to A will be covered and what will be seen is but the silhouette of the support of the invariant measure. This is in fact how the image on the left part of Fig. 4 was obtained.

3. ITERATED FUNCTION SYSTEMS WITH CONDENSATION

There exists an extension of the theory of the iterated function systems which is of particular importance to what we are aiming to present. One may assume, namely,

that one of the transformations of an *X.IFSP*, let us denote it w_0, has a particular property - it transforms the whole space X into a compact subset C of it according to a the following rule:

$$w_0: x \to w_0(x) = \text{random}(C) \tag{14}$$

where by random(C) we denote a point chosen at random from set C. As shown by Barnsley, essential theorems of the iterated function systems preserve their validity, as the condensation transformation is allowed to enter the set of iterated functions. For our purposes, one particular form of the condensation transformation is of major importance. We assume that the condensation set consists of but one point $C = P \in X$. In this case, obviously, the condensation rule becomes even more simple:

$$w_0: x \to w_0(x) = P\,, \tag{15}$$

In what follows, X will be always a plane equipped with the Euclidean metric and a Cartesian coordination frame. We shall also assume that P is located at the origin of the frame: $P = (0, 0)$. In such a case, transformation w_0 can be considered as the limit of an affine transformation in which all its scaling, rotation and translation parameters were brought to 0.

How an IFSP with condensation behaves under the application of the random iteration algorithm we shall discuss in chapter 5.

4. QUASICRYSTALS AND THEIR DIFFRACTION PATTERNS

The ideal infinite n-dimensional crystal is an object built from a finite number of identical elements in such a way that it stays invariant under translations whose vectors belong to a countable set of (integer coefficients) linear combinations of n elementary vectors – a lattice. The matter density function of a crystal can be expanded in a Fourier series. The Fourier transform consists of point sharp peaks whose positions belong to another countable set of (integer coefficients) linear combination of n elementary vectors – the reciprocal lattice. Translational symmetry puts a strong restriction on all other possible elements of the symmetry of a crystal. In particular, its rotational symmetry axis can be but two-, four- or sixfold. All other kinds of rotational symmetry are strictly forbidden.

Does any object whose Fourier transform consists of sharp peaks display the translational symmetry? The answer is – no. The Penrose tilings [5] make the simplest, but nontrivial example. As demonstrated in 1982 by Alan Mackay, this man made, plane filling structure, built but from two kinds of rhombi, lacks the translational symmetry, but its diffraction pattern displays sharp peaks and, what makes it even more beautiful, contains a clear fivefold rotational symmetry axis [6].

There exist uncountably many versions of the Penrose tiling. They are all different globally, yet any finite piece of each of them can be found in any other.

Objects, which lacking the translational symmetry display sharp peaks diffraction patterns were found in physics laboratories. In 1984, Shechtman, Blech, Gratias and Cahn published first diffraction patterns (of a rapidly cooled AlMn alloy) which displayed the forbidden fivefold symmetry axis [7]. Since this discovery, more than 600 papers were published on the new class of materials, commonly referred to as quasicrystals [8]. Most quasicrystalline materials are produced by nonequilibrium technologies such as quenching. From the thermodynamic point of view they are metastable i.e. when heated change their structure into one translationally invariant lattices. There exist, however, few examples of quasicrystals which are stable thermodynamically and be grown up to the size of several millimetres. The diffraction patterns of all the materials display one of the forbidden rotational symmetries.

In what follows we shall look into the possibility of using the iterated function system technique to produce patterns of quasicrystalline symmetry.

5. CAN ITERATED FUNCTION SYSTEMS BE USED TO PRODUCE QUASICRYSTALLINE PATTERNS?

One of the most remarkable and pleasant features of the Barnsley algorithm is a smooth dependence of the shape of set A on the parameters of the iterated function system *A.IFS* for which the set is the attractor. This is stated formally in by the following theorem (see Ref. [2]):

Theorem 5.1

Let $A.IFS = \{w_1, w_2, w_3, \ldots w_n\}$ be an iterated function system of contractivity s defined in a complete metric space (X, d). Let all of its transformations w_α, $\alpha = 1, 2, \ldots, n$, depend continuously on a parameter $p \in P$, where P is a compact metric space. Then the attractor $A(p)$ depends continuously on p with respect to the Hausdorff metric $h(d)$.

What it means in practice one can easily imagine. If within a numerical procedure one starts varying in a smooth manner parameters of the transformations which define *A.IFS*, one will observe on the computer graphics display a smooth variation of its attractor. Performing a systematic study of this phenomenon we arrived in one of the computer runs to the limits of validity of the Barnsley algorithm. The limit has proven to be very interesting. See Fig. 7. It presents a sequence of attractors of a particular iterated function system with probabilities, let us denote it by *Q(s).IFSP*, which consists of five affine transformations and five probabilities $\{w_0, w_1, w_2, w_3, w_4; p_0, p_1, p_2, p_3, p_4\}$. Since any affine transformation can be represented by a sequence of : a scaling (s_x, s_y), a rotation (ϕ_x, ϕ_y) and a translation (t_x, t_y), we shall

in what follows describe the transformations by giving all six parameters of the three components. In the particular case of *Q(s).IFSP* the values of the parameters are as follows:

$$t_{x,0} = t_{y,0} = 0 \tag{16}$$

$$s_{x,0} = s_{y,0} = s_0 \quad \text{where} \quad 0 \le s_0 \le 1 \tag{17}$$

$$\phi_{x,0} = \phi_{y,0} = 0 \tag{18}$$

$$p_0 = \varepsilon, \quad \text{where} \quad 0 \le \varepsilon \le 1 . \tag{19}$$

$$t_{x,i} = (1/4)\cos(2\pi i/4) , \tag{20}$$

$$t_{y,i} = (1/4)\sin(2\pi i/4) , \tag{21}$$

$$s_{x,i} = s_{y,i} = s , \quad \text{where} \quad 0 \le s \le 1 , \tag{22}$$

$$\phi_{x,i} = \phi_{y,i} = 0 , \tag{23}$$

$$p_i = (1 - \varepsilon)/4 , \quad \text{for} \quad i = 1,2,3,4 ,$$

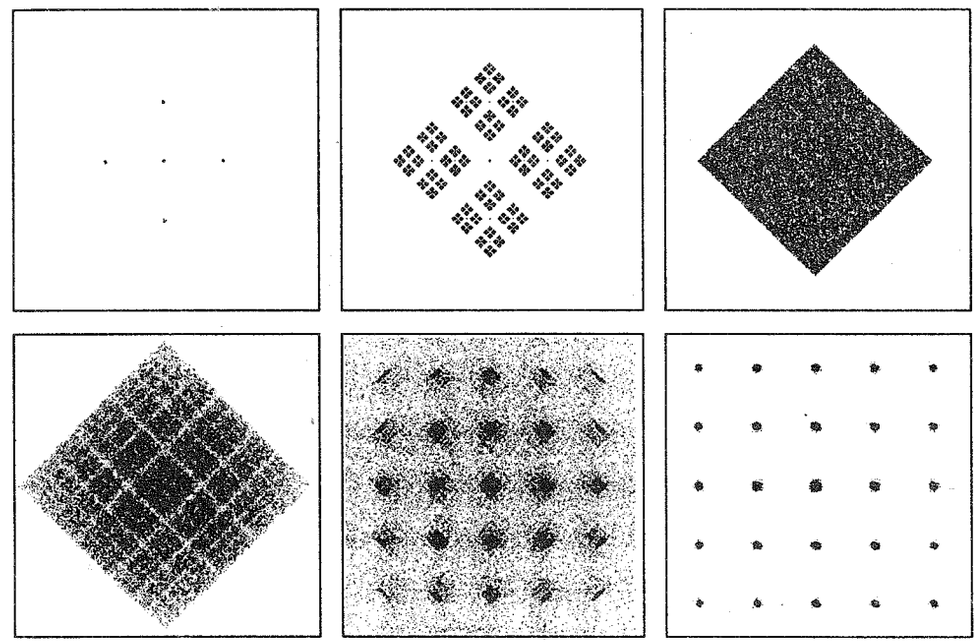

Fig. 7. Images of the invariant measures of the *Q(s).IFSP*. Scaling factor s was equal 0.01, 0.4, 0.5, 0.6, 0.95 and 1.0, respectively, for consecutive figures (starting at the upper left corner). Scaling factor s_0 for the central function was equal 0.01 and its probability ε was equal 0.1.

Figure 7 presents a sequence of attractors of the $Q(s).IFSP$ for a few values of s which determines the contractivity factors of the four, non-zero translation transformations of the IFSP: w_1, w_2, w_3 and w_4. The scaling factor of the w_0 transformation was set equal to 0.01. It is rather awkward to present invariant measures, when w_0 is indeed a condensation to a single point. The computer graphics images are in such a case built from separate, single pixels which makes them very difficult to reproduce.

For $s = 0.5$, Fig. 7c the attracting set makes a square oriented with its diagonals along the translation vectors defined by Eqs (20, 21).

As s goes below this critical value, the attractor becomes totally disconnected. As s decreases, the scale of its self-similar details shrink, what makes them one by one disappear from the computer graphics display, but from the formal point of view nothing of this kind really happens. In the limit $s = 0$, however, a real transition occurs: all four transformations $w_1,...,w_4$ become singular and define four condensation points located at points determined by the translation vectors. Thus, the attractor of $Q(0).IFS$ consists of but five points:

$$P_i = (t_{xi}, t_{yi}) , \; i = 1,2,3,4,5 \tag{25}$$

and all invariant measure is concentrated on them.

Using the Dirac delta function we may write the measure as a sum of five such deltas whose amplitudes are defined by the set of probabilities of $Q.IFSP$:

$$\mu_{Q(0)} = \sum_{i-1}^{5} p_i \delta(\vec{r} - \vec{t}_i) \tag{26}$$

A similar story happens at the other end of the s validity range. For $s > 0.5$ the attractor of $Q(s).IFS$ is no more disconnected - it becomes overlapping, but as long as $s < 1$ it is bounded. Its actual size depends on the value of the translation vectors and s. As s becomes equal 1, the four transformations w_1, w_2, w_3, w_4, which depend on it, are no more contractive. The system leaves the range of validity of the theorems discussed above, but still, as Fig. 7f indicates it, the structure of the invariant measure simplifies considerably. Now, most of the invariant measure becomes concentrated around vortices of a square lattice locked at the condensation point (0, 0) defined by transformation w_0. The peaks of the invariant measure presented in the figure are smooth, due to the finite value of the s_0 scaling parameter, which, as explained above, we have set for practical reasons. When, however, $s_0 = 0$, once more the measure becomes singular and can be represented as an infinite sum of Dirac delta functions localised at the vortices of the square lattice defined by transformations w_1, w_2, w_3, w_4 , which at the $s = 1$ limit become pure translations:

$$\mu_{Q(1)} = \sum_{k=1}^{\infty} \rho_k \delta(\vec{r} - \vec{r}_k) \tag{27}$$

where vectors $\vec{r}_k$ indicate positions of all vortices of the square lattice. The meaning

of the amplitudes ρ_k is essential. As one can guess, the random iteration algorithm applied to $Q(1).IFSP$ produces a kind of a random walk on a square lattice. Four possible directions and the step length of the walk are determined by the translation vectors of transformations w_1, w_2, w_3, w_4. Their probabilities are determined by p_1, p_2, p_3 and p_4 which do not, however, sum up to unity, since there exists a non zero probability of choosing the condensation function w_0, what in terms of the random walk means that the walker with non-zero probability is from time to time brought to the starting point. Amplitudes ρ_k describe the probability that the random walker visits vortex number k. Due to the existence of the condensation transformation, which with probability $p_0 = \varepsilon$ makes the random walker to return and start its walk from beginning, the invariant measure is not smeared out onto the whole lattice but remains well localised on vortices close to the origin. Values of ρ_k decay fast with the distance from the central point. Thus, the sum

$$\sum_{k=0}^{\infty} \rho_k \quad \text{remains finite } (= 1) .$$

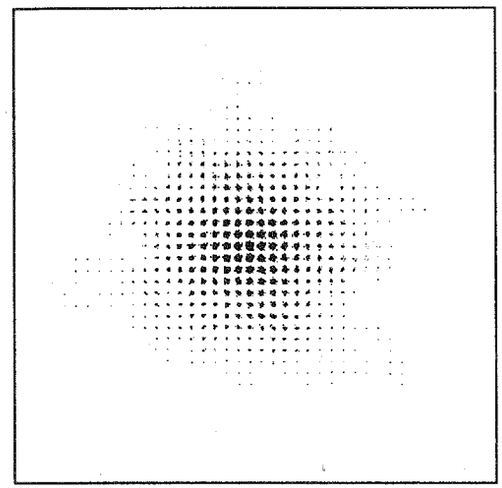

Fig. 8. A larger part of the invariant measure of $Q.IFS$ obtained in the $s = 1$ limit. s_0 was set equal to 0.03 to visualise those points of the lattice which in the random iteration procedure were visited more often.

Obviously, in the $s = 1$ limit, transformations w_1, w_2, w_3 and w_4 are no more contractive, consequently, the Barnsley theory is no more valid. Yet, as shown above, the invariant measure exists and displays nice, from the point of view of a physicist, properties. We shall not look into the details of the formal theory of such IFS-s but we shall rather exploit them to describe objects interesting from the point of view of a physicist.

Looking at figures and one may ask oneself a general question:

Which is the form of the invariant measure for an IFSP built from, say n = 3, 4, 5, 6, 7 ... symmetrically distributed translations and 1 condensation transformation?

Vectors of the *symmetrically distributed translations* are given by:

$$t_{x,i} = a\cos(\frac{2\pi i}{n}) \qquad t_{y,i} = a\sin(\frac{2\pi i}{n}) \tag{28}$$

where a is the magnitude of the translation vectors and n is their number.

Even without trying, one would replay that for $n = 3$ and 6 the invariant measure should be concentrated on vortices of a triangular lattice, which indeed is the case. See Fig. 9

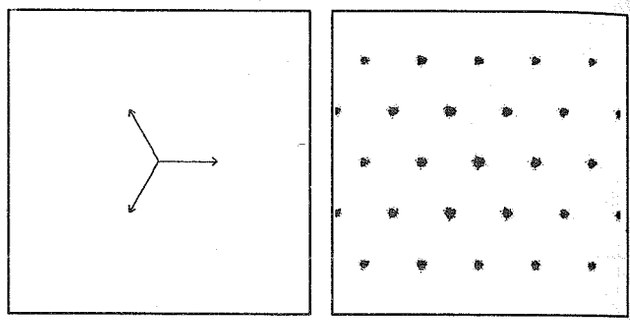

Fig. 9. Invariant measure for an IFSP built from three translations w_1, w_2, w_3 and one strong contraction w_0.

As previously, we have put the scaling factor s_0 of w_0 equal to 0.01 to make the image better visible. For $s_0 = 0$, but a triangular lattice would be seen.

Results of the above calculation could be predicted. But, what happens when the angle between the translation vectors is neither any multiplicity of 2/2, 2/3 or 2/4? Fig. 10. presents the simplest $n = 5$ case.

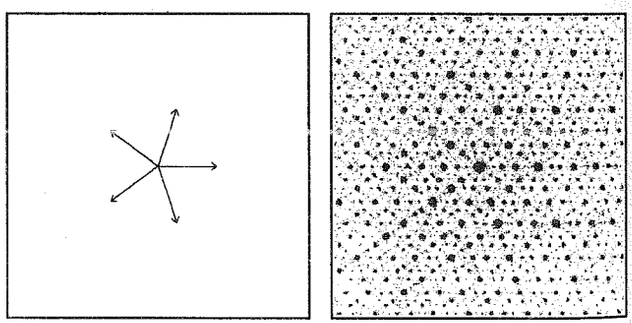

Fig. 10. The case of an IFSP built from five translations w_1, w_2, w_3, w_4, w_5 and one strong contraction w_0 for which $s_0 = 0.01$ and $p_0 = 0.1$.

As easy to see, the fivefold symmetry of the star made by the translations vectors of the IFS induces the same type of symmetry for the invariant measure. And this is a general rule. Figure 11 presents a few next cases.

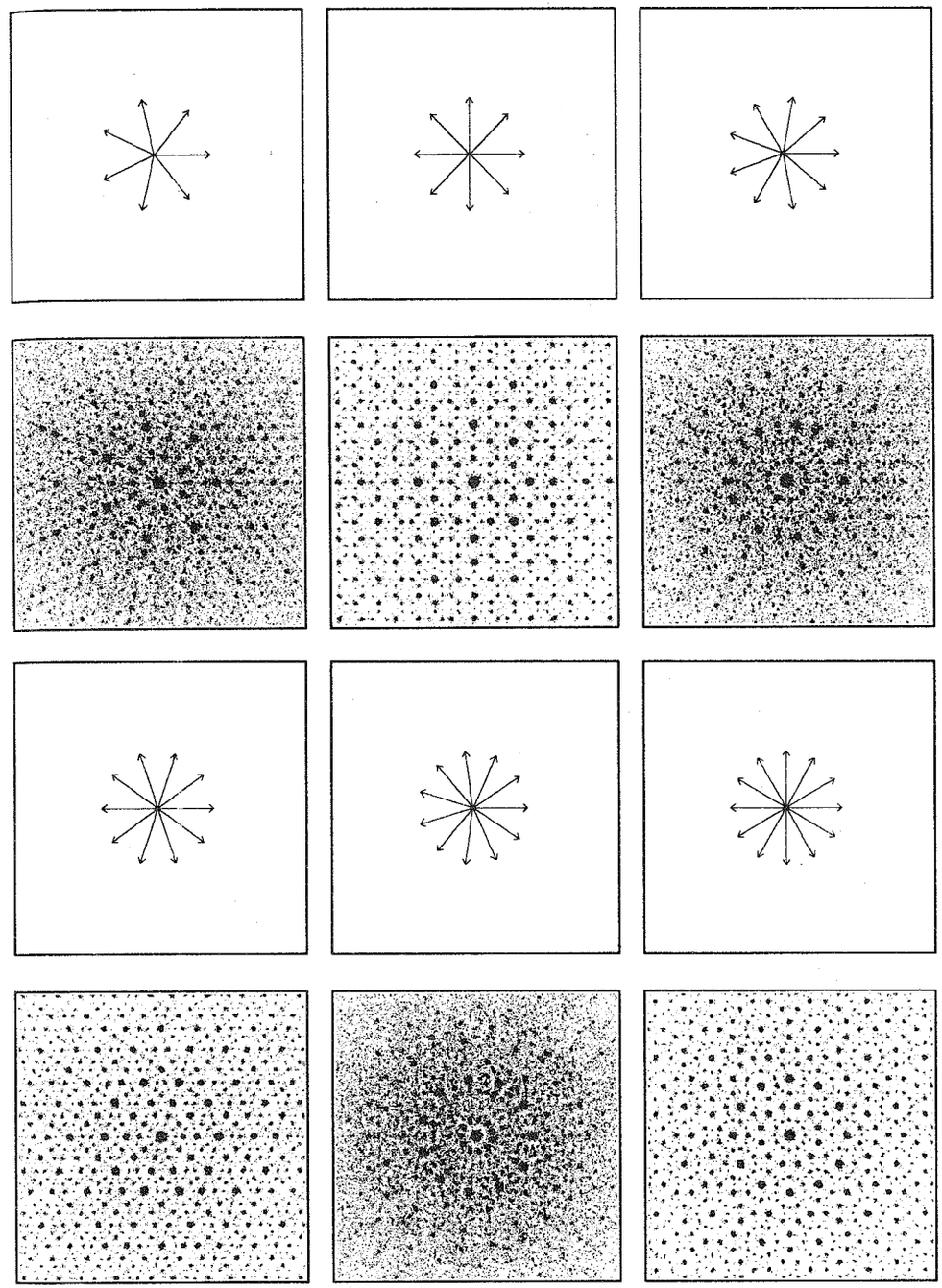

Fig. 11. Central parts of a few IFSP-s built on symmetrical systems $\{w_1, w_2, ..., w_n\}$, $n = 7, 8, ..., 12$, of elementary translations. The additional, strongly contractive transformation w_0 was in all presented cases the same: $s_0 = 0.01$, $p_0 = 0.1$.

Let us discuss in more detail the structure of images presented in Fig. 11. The random iteration procedure applied to the particular IFSP-s, in which one transformation is contractive and all others are (distance and area preserving) translations, produces a random walk (with returns occuring with probability determined by p_0) on the sets of points to which one may get using the elementary translations. The structure of such sets, let us denote them by Q_n depends obviously on n. In a few cases the structure is particularly simple: Q_2, Q_3, Q_4 and Q_6 have the form of regular lattices. In all other cases, sets Q_n are dense in the plane, yet as clearly seen from Fig. 11, in a computer run not the whole plane becomes evenly covered. On the contrary, the density with which the points produced by the random iteration procedure cover the plane displays a clear hierarchy: apparently some of the points from Q_n are more often visited then others. The explanation of the fact is rather simple. Firstly, probability that the random walker arrives to some of the points is very low, since to arrive to them the walker must perform (without any return) a large number of steps which may be difficult in view of the finite probability of transformation w_0 , which brings the walker to the starting point. Secondly, to all points of Q_n one may arrive by more than one path. In what follows we shall consider the two problems in more detail. To fix attention we shall illustrate some partial solutions with the case Q_{10}, most interesting from the point of view of a physicist.

6. RANDOM WALKER MODEL FOR INVARIANT MEASURES OF Q_n. *IFSP*

The basic questions are as follows:

1. Which is the probability that the random walker has made k steps without any return?

2. To which points of the plane can random walker arrive with k-steps?

3. How many different k-step paths lead from the starting point to each of such points?

We start with question 1. To answer it, let us imagine that a large number, say N, of random walkers start a walk. The probability that they will make the first step is equal $(1 - p_0)$. Thus, after the first step of the iteration procedure we shall find

$$N_0^{(1)} = p_0 N \tag{29}$$

walkers remaining at the starting point, since they have chosen transformation w_0. Each of the remaining once

$$N_1^{(1)} = (1 - p_0)N \tag{30}$$

have chosen one of the n translations and is found standing at one of those points of

Q_n to which one may arrive with but one step. Let us denote this subset $Q_{n,1}$.

In the next step of the iteration procedure, the situation will be more complex. The number of walkers found at the starting point will be equal:

$$N_0^{(2)} = p_0 N_0^{(1)} + p_0 N_1^{(1)} = p_0^2 N + p_0(1 - p_0)N \tag{31}$$

since $p_0 N_0^{(1)}$ of them were unlucky enough to choose w_0 for the second time while $p_0 N_1^{(1)}$ were hit by the bad luck for the first time.

The number of those distributed among points of $Q_{n,1}$ will be equal:

$$N_1^{(2)} = (1 - p_0)N_0^{(1)} \tag{32}$$

since we find here only the walkers which have freshly arived from the starting point; those which stayed here previously either have returned to the starting point (already considered) or went one step forward to the subset $Q_{n,2}$:

$$N_2^{(2)} = (1 - p_0)N_1^{(1)} = (1 - p_0)^2 N \tag{33}$$

In general, after the i-th step of the iteration procedure populations of walkers at consecutive levels $Q_{n,k}$, to which they have arrived arrive, will be given by:

$$N_0^{(i)} = p_0 \sum_{k=0}^{i-1} N_k^{(i-1)}$$
$$N_k^{(i)} = (1 - p_0) N_{k-1}^{(i-1)}, \quad k = 1,2,...,i \tag{34}$$

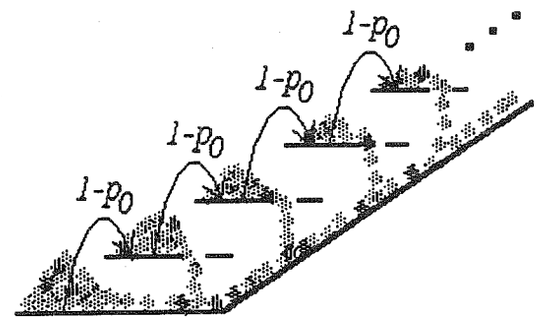

Fig. 12. Schematic representation of the random walkers problem. They either go up along the lader of $Q_{n,k}$, and this happens with probability $(1 - p_0)$, or with probability p_0 fall back to the starting point.

Thus, after the i-th iteration, all levels up to the i-th one will be populated. See Fig. 12.

In the limit of infinite number of iterations a stationary state is assymptotically reached. At this state all populations remain constant i.e. are invariant under the application of rule (34). Thus we have:

$$N_0^{\infty} = p_0 \sum_{k=0}^{\infty} N_k^{\infty}$$
$$N_k^{\infty} = (1 - p_0)N_{k-1}^{\infty}, \quad k = 1,2,...,i \tag{35}$$

Since

$$\sum_{k=0}^{\infty} N_k^{\infty} = N$$

at this state populations of consecutive levels are given by:

$$N_0^{\infty} = Np_0 = Nq_0$$
$$N_k^{\infty} = Np_0(1-p_0)^k = Nq_k, \quad k = 1,2,3... \tag{36}$$

where, by

$$q_k = \frac{N_k^{\infty}}{N} = p_0(1-p_0)^k \tag{37}$$

we denoted the stationary probability that a random walker can be found at the k-th level of the walk i.e. at a point located within subset $Q_{n,k}$.

Each of subsets $Q_{n,k}$ (except $Q_{n,0} = \{(0, 0)\}$) contains more than one point and the $N_{k,\infty}$ walkers must be distributed between them. See Fig. 13.

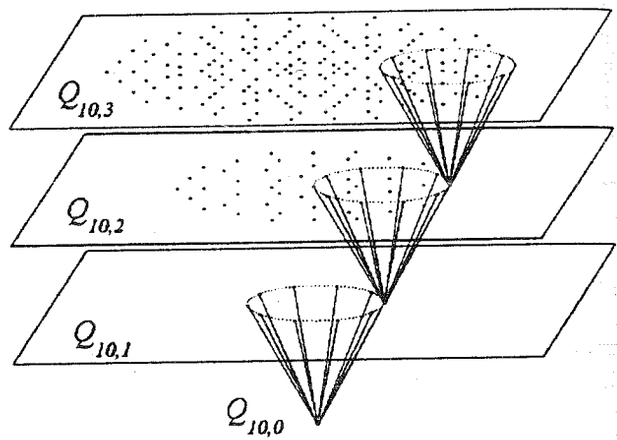

Fig. 13. Structure of subsets $Q_{n,k}$ for the $n = 10$ case, $k = 1, 2, 3$. Points connected with the dotted line can be reached from a single point belonging to the previous level.

The distribution of walkers among the points from a level $Q_{n,k}$ is governed by the ratio of different paths via which a walker can arrive to a given point P_i, we denote it by $m_{n,k}(P_i)$, to the total number of paths $M_{n,k}$, which lead to the k-th level:

$$r_{n,k}(P_i) = \frac{m_{n,k}(P_i)}{M_k}, \quad i = 1,2,...,L_{n,k},$$
$$\text{where} \quad M_k = \sum_{i-1}^{L_{n,k}} m_{n,k}(P_i), \quad k = 1,2,3,... \tag{38}$$

From the point of view of the complete random walker problem, the ratio is equal to the conditional probability that, having arrived to the k-th level, the walker finds itself in a concrete point P_i. By $L_{n,k}$ we denoted here the number of points within subsets $Q_{n,k}$, i.e. the number of points to which the walker can arrive in exactly k steps.

Finding numbers $m_{n,k}(P_i)$ and $M_{n,k}$ analytically is probably not easy. On the other hand, a numerical procedure which determines them is rather simple.

Knowing the probabilities q_k of arriving to the k-th level and the conditional probabilities $r_{n,k}(P_j)$ one can find the total probability $R(P_j)$ that a walker is found in point P_j. One needs just sum up contributions coming from all levels within which the points is accessible by at least one path:

$$R_n(P_j) = \sum_{k=0}^{\infty} q_k r_{n,k}(P_j), \quad j = 1,2,3,... \tag{39}$$

Note, that the sum starts with $k = 0$ to include into the consideration also the starting point $P_1 = (0, 0) = Q_{n,0}$. Note also, that we have changed the variable which indexes points within Q_n which is equal to the sum of all subsets $Q_{n,k}$:

$$Q_n = \bigcup_{k=0}^{\infty} Q_{n,k} \tag{40}$$

In a numerical calculations, set Q_n is updated in steps as consecutive sets $Q_{n,k}$ are found numerically.

Returning back to the formalism of the iterated fuunction systems with probabilities we conclude, that the invariant measure for the $Q_n(\varepsilon)$.IFSP is an infinite sum of Dirac deltas whose amplitudes are given by probabilities $R_n(P_j)$:

$$\mu_{Q_n} = \sum_{j=1}^{\infty} R_n(P_j)\delta(\vec{r} - \vec{r}_j), \quad j = 1,2,3,... \tag{41}$$

The amplitude of the delta function localized at a paricular point P_i depends basically on the length l of the shortest paths via which a random walker can arrive to it. When l is large, i.e. point P_i is found for the first time within $Q_{n,l}$, then R_n is certainly small. The decay of the probability with l depends obviously on p_0. For $p_0 \to 1$ all $R_n \to 0$.

7. ITERATED FUNCTION SYSTEMS WITH CONDENSATION AND BONDS

The problem of a random walk with return on sets Q_n can be modified in a manner that proves very useful in possible applications of IFSP-s to describe quasicrystalline diffraction patterns. Namely, one may assume that any walker is not allowed make more than K steps without return, i.e. if one was lucky enough not to choose condensation transformation w_0 for K consecutive times, then next time he is forced to choose it. See Fig. 14.

Such a limit put on the walkers modifies values of the stationary populations reached in the limit of infinite iterations. As easy to check, now we have:

$$N_0^{\infty} = N\{\sum_{k=0}^{K}(1-p_0)^k\}^{-1}$$
$$N_k^{\infty} = N_0^{\infty}(1-p_0)^k, \quad k = 1,2,3,\ldots,K \tag{42}$$

What happend here, in comparison with the unlimited walk case, is that the shape of the population distribution is preserved, but the absolute values are different since N walkers must be now distributed but on a finite number of levels.

A probability to find a walker at the i-th level is now given by:

$$q_0 = \{\sum_{k=1}^{K}(1-p_0)^k\}^{-1},$$
$$q_k = q_0(1-p_0)^k, \quad k = 1,2,\ldots,K \tag{43}$$

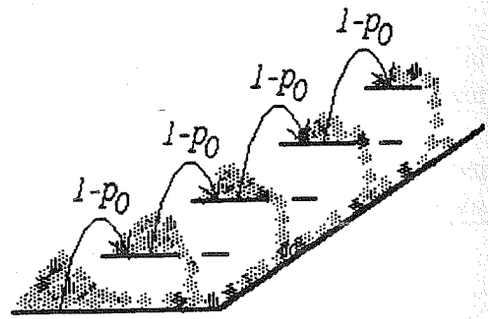

Fig. 14. Random walker model with a bond. Any of the walkers cannot make more than K steps. After the K-th step it is forced to return to the starting point.

The rest of the reasoning goes along the same path as we presented it for the unlimited walker case. Except for the limit put now on values of k, equations (38), (39) preserve their validity. Eq. (40) turns now into a definition of a finite part of Q_n:

$$Q_n^{(K)} = \bigcup_{k=0}^{K} Q_{n,k} \tag{44}$$

The number of points in any of the $Q_n^{(K)}$, $K = 1, 2, 3\ldots$, sets is finite. See Figs 15 and 16. As a result, the number of Dirac delta functions in Eq. (41) also becomes finite and computer graphics images of such invariant measures are much simpler. Fig. 17 presents a few examples. In all presented cases the largest number of steps K a random walker may make without any return was put equal to 5 except for the last image for which $K = 4$. Probability of transformation w_0 was set equal to 0. The amplitude of the delta functions are in the figure coded as the surface of circles whose centers are localized in points belonging to $Q_n^{(K)}$. As clearly seen, the function located at the origin has the largest amplitude. There are two reasons for that. First of all, this single point is the only member of the whole $Q_{n,0}$ set from which all radom walkers

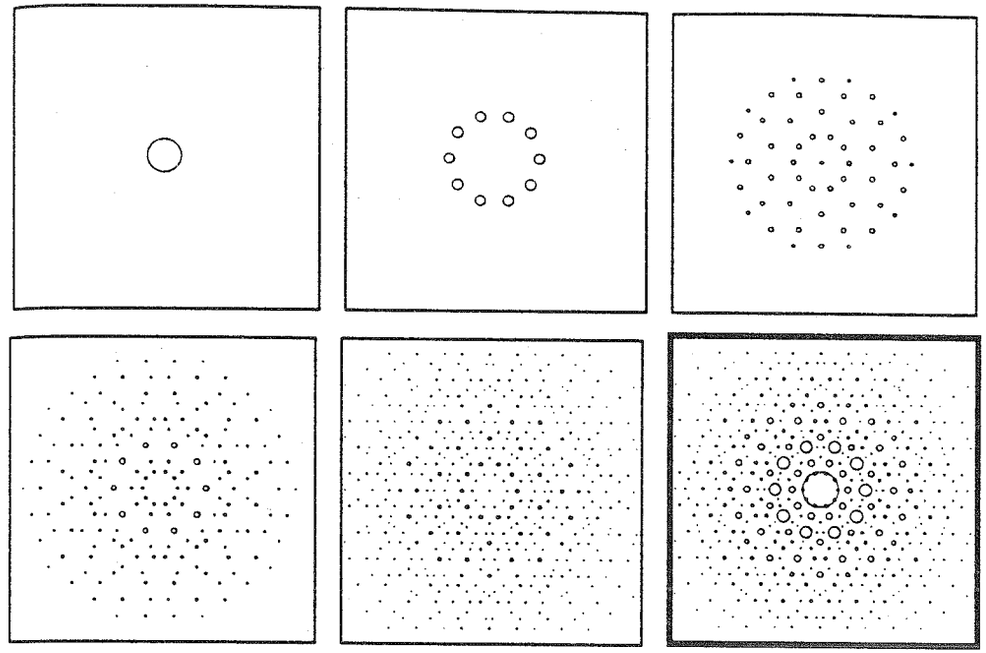

Fig. 15. Contribution of consecutive $Q_{n,k}$, $n = 10$, $k = 0, 1, 2, 3$, to the invariant measure of the Q_{10}-*IFSP* with a bond $K = 4$. $p_0 = 0$. The invariant measure itself is shown in the last (thick) frame.

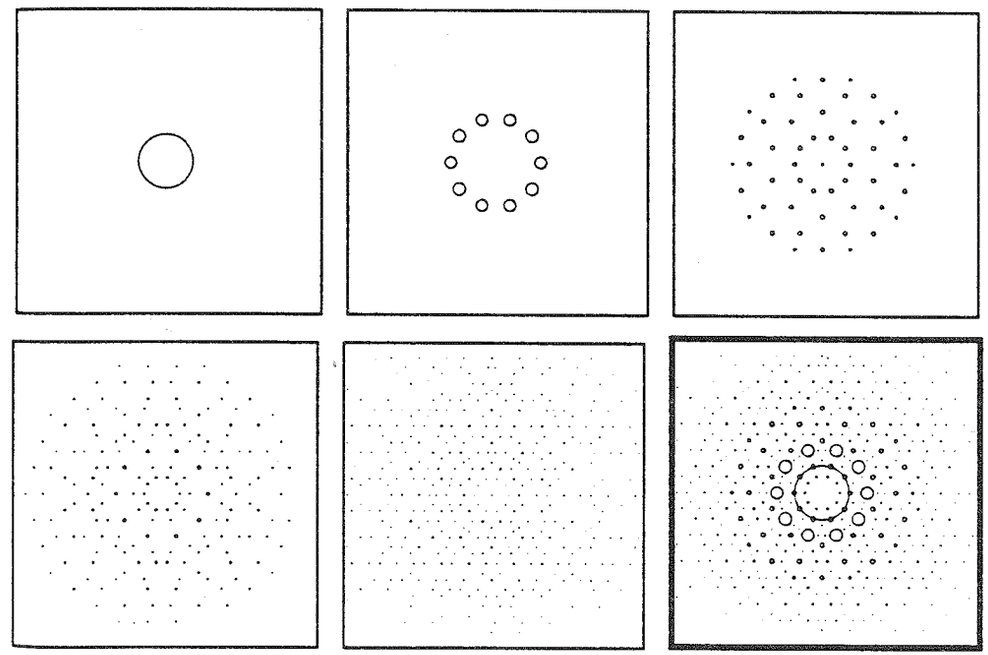

Fig. 16. Contribution of consecutive $Q_{n,k}$, $n = 10$, $k = 0, 1, 2, 3$, to the invariant measure of the Q_{10}-*IFSP* with a bond $K = 4$. $p_0 = 0.5$. In contrast to Fig. 15, $p_0 = 0.5$.

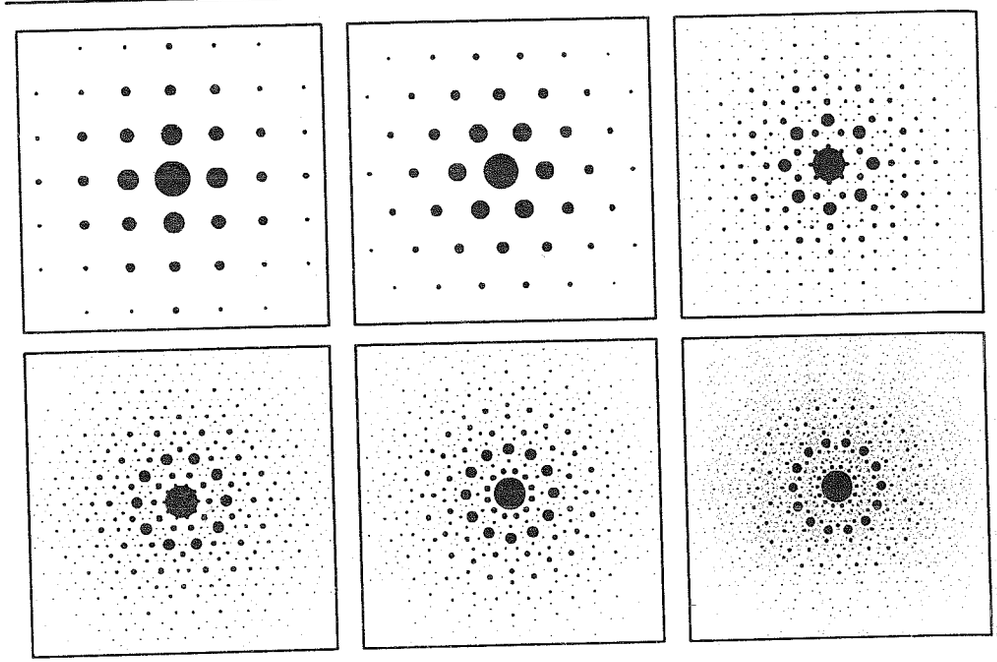

Fig. 17. Invariant measures for Q_n.*IFSP*-s with a bond calculated according to the random walk model. $n = 4, 6, 8, 10, 12, 14$.

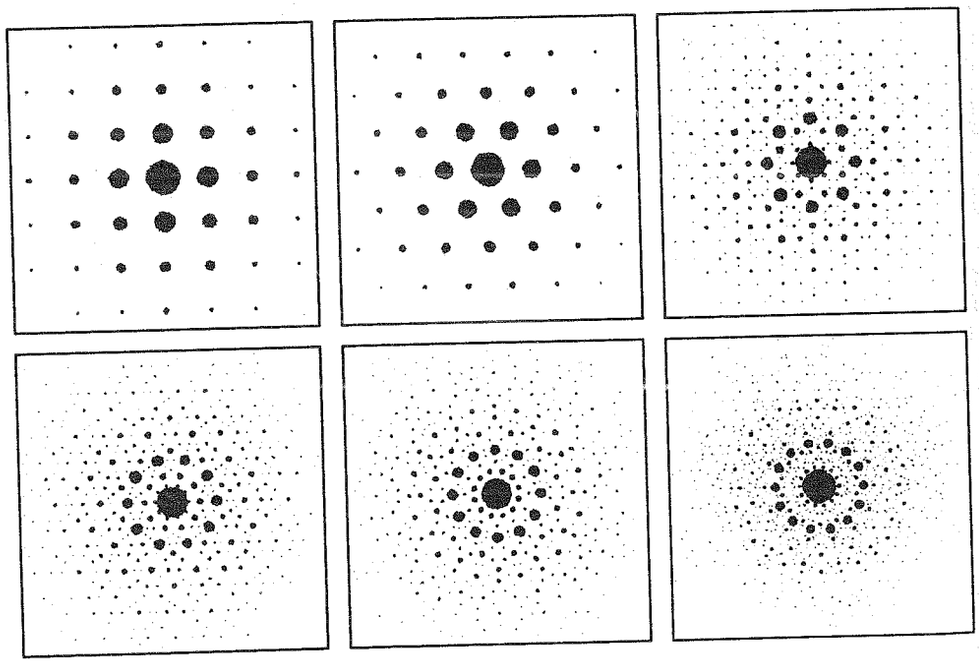

Fig. 18. Invariant measures for Q_n.*IFSP* with a bond $K = 5$ (4 for the last image) obtained by means of the random iteration procedure. $n = 4, 6, 8, 10, 12, 14$.

start and the probability to find a walker at the level is equal $q_0 > q_1 > q_2 \ldots$ according to Eq. (43). Secondly, point (0, 0) belongs also to all sets $Q_{n,m}$, $m > 1$ (it does not belong to $Q_{n,1}$) and thus the probability in question is still higher. Fig. 18 presents images of invariant measures obtained by means of the random iteration procedure. Probability p_0 of the condensation transformation w_0 was set equal to 0. Number of pixels drawn around centers where the invariant measure is nonzero is equal to the number of times which the iterated point visited each of the centers. Comparison of Figs. 17 and 18 proves that the random walker model works very well.

8. QUASICRYSTALLINE PATTERNS FOR IFSP-s CONSISTING OF BUT CONTRACTIVE TRANSFORMATIONS

As mentioned above, simple interpolation allows one to create IFSP-s which in a smooth manner join two arbitrary invariant measures. Many interesting phenomena can be observed on the graphics display when such interpolations are performed for IFSP-s used to produce the diffraction quasicrystalline patterns.

Let $Q_{10}(s)$.IFSP denote a continuous family of IFSP-s built on ten symmetrically oriented affine transformations $\{w_1(s), w_2(s),\ldots,w_{10}(s)\}$ with the scaling parameter $0 \le s \le 1$ and one strongly contractive (in the limit: condensing) scaling transformation $w_0(s_0)$. For $s = 0$, the 10 transformations turn into condensations to 10 symmetrically distributed single points as shown in Fig. 19.

For $s = 1$, $s_0 = 0$, the IFSP turns into one of the particular IFSP-s which produce the singular quasicrystalline measures. Looking carefully at the images of invariant measures produces by the IFSP for $0 < s < 1$ one may notice that at $s \approx 0.618$ a well defined pattern appears on the graphics display. See Fig. 19. Since in this case

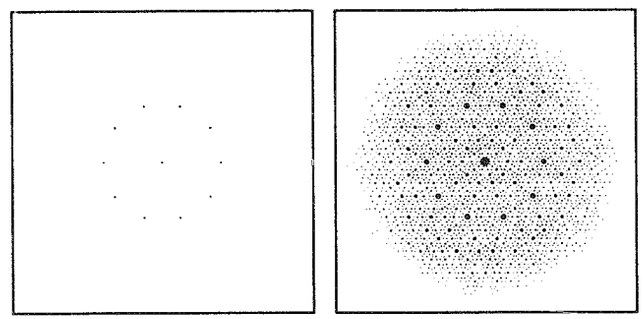

Fig. 19. Invariant measures of the $Q_{10}(s)$.IFSP with a bond $K = 5$ for $s = 0$ and $s = \dfrac{\sqrt{5} - 1}{2}$.

all transformations are contractive, all theorems of the Barnsley theory apply. The observed invariant measure has a compact support. Unfortunately, intensities of its peaks are not in even a qualitative accordance with those of a quuasicrystalline diffraction pattern.

CONCLUSIONS

Quasicrystalline diffraction patterns belong to most rich geometrical objects. Bragg reflections within any finite piece of such a pattern are located on an infinite set of points. At the first sight any attempt to reproduce them with a simple algorytm should be futile. The study we presented proves that this is not necessarily the case. As demonstrated, the technique of iterated function systems is versatile enough to reach the aim, at least in the qualitative terms. Invariant measures of some particular iterated function systems with probabilities which we constructed display a strong similarity to the images of the diffraction patterns obtained in real experiments. In the ideal case the invariant measures can be expressed as sums of an infinite number of Dirac delta functions. Their amplitudes can be calculated using notions of the random walk theory. The orderings of the amplitudes and that of the Bragg reflections are in qualitative agreement. A quantitative analysis of the problem needs still some more work.

Acknowledgements: All numerical work described in the paper, in particular generation of the fractals presented in the figures, was performed on computers purchased under KBN Project 2 2439 92 03.

The visit of Piotr Pierański to the University of Calabria was sponsored by the European Economic Community under Contract ERB-CIPA-CT-92-2251. P.P. thanks Simonetta and Roberto Bartolino, for help and hospitality.

Discussions with Elisabeth Dubois-Violette and K. W. Wojciechowski are gratefully acknowledged.

(Received 18 January 1995)

References

[1] B. Mandelbrot, Fractals: *Form, chance, and dimension*, San Francisco, W. H. Freeman & Co. (1977).
[2] M. Bransley, *Fractals Everywhere*, Academic Press (1988).
[3] All images of fractal attractors presented in the paper were obtained with the use of the *Fractal Object Editor*, by P. Pierański and R. Barberi.
[4] See: Tom Lindstrom, *Nonstandard approach to interated function systems*, p. 86 in *Nonstandard Methods in stochastic and mathematical physics*, eds. S. Albeveiro, J. E. Fenstad, R. Hregh-Krohn and T. Lindstom. Academic Press, New York (1986).
[5] R. Penrose, Bull. Inst. Math. and its Appl., **10**, 266 (1974).
[6] A. L. Mackay, Physica **114A**, 609 (1982).
[7] D. Shechtman, I. Blech, D. Gratias, J. W. Cahn, Phys. Rev. Lett. **53**, 1951 (1984).
[8] For a review, see e.g. T. Janssen, Phys. Rep., **168**, 55 (1988).